Adsorption Equilibria and Kinetics of Carbon Monoxide on Zeolite 5A, 13X, MOF-5, and MOF-177

Dipendu Saha and Shuguang Deng*

Chemical Engineering Department, New Mexico State University, Las Cruces, New Mexico 88003

Carbon monoxide adsorption equilibria and kinetics on zeolite 5A, 13X, MOF-5, and MOF-177 were measured volumetrically at (298, 237, and 194.5) K and carbon monoxide pressures up to 108 kPa. It was found that zeolite 5A had the highest adsorption capacity at ambient temperature (298 K) and ambient pressure (108 kPa), whereas MOF-177 was a better adsorbent at (194.5 and 237) K. Both the Langmuir and Freundlich isotherm models were used to correlate the adsorption isotherms. Diffusivities of carbon monoxide in these adsorbents were estimated from the adsorption uptake curves by a micropore diffusion model. The average carbon monoxide diffusivities at 298 K and carbon monoxide pressures below 108 kPa are $3.42 \cdot 10^{-11}$ $m^2 \cdot s^{-1}$, $1.40 \cdot 10^{-11}$ $m^2 \cdot s^{-1}$, $1.72 \cdot 10^{-8}$ $m^2 \cdot s^{-1}$, and $5.01 \cdot 10^{-9}$ $m^2 \cdot s^{-1}$ for zeolite 5A, 13X, MOF-5, and MOF-177, respectively. The heat of adsorption of carbon monoxide at low coverage on zeolite 5A and 13X is below 70 $kJ \cdot mol^{-1}$ and drops rapidly as the coverage increases, while the heat of adsorption of carbon monoxide in MOF-5 and MOF-177 is in the range of (16 to 22) $kJ \cdot mol^{-1}$.

1. Introduction

Carbon monoxide (CO) is a colorless, odorless, tasteless, and highly toxic gas. It is a major industrial gas that has many applications in bulk chemicals manufacturing. Carbon monoxide is widely used in the production of methanol through hydrogenation, liquid hydrocarbon fuels in the Fischer−Tropsch process, and acetic acid by reaction with methanol. Carbon monoxide is typically produced through partial oxidation of carbon-containing compounds.[1] Carbon monoxide is toxic to human beings because it combines with hemoglobin in the blood to form carboxy-hemoglobin that reduces the oxygen carrying capacity of blood and leads to death. So it is imperative to remove even a trace amount of carbon monoxide in air streams for safety considerations. Carbon monoxide is the major component of syngas produced in the methane−steam reforming process, which is often used for power generation. If the hydrogen in syngas is used for electricity generation in proton-exchange membrane fuel cells, carbon monoxide in hydrogen must be removed to below 0.2 ppm to protect the platinum electrocatalyst.[2,3] So, production of ultrapure fuel cell grade hydrogen is an emerging challenge and opportunity for industrial gas business.

Studies on carbon monoxide separation from gases began as early as World War I.[1,4,5] Most of the processes involve numerous kinds of catalysts that can directly oxide carbon monoxide to carbon dioxide or chemically adsorb carbon monoxide on the catalyst surface. The metals that can chemically adsorb carbon monoxide include copper,[6] palladium,[7] cobalt,[8] or even gold.[9] The catalysts that were evaluated for their catalytic activity for converting carbon monoxide to carbon dioxide include lithium doped nickel oxide-silica,[10] metallophthalocyanine monolayers supported on graphite,[11] potassium carbonate promoted iron,[12] magnesium oxide,[13] or zinc oxide.[14]

* Corresponding author. Phone: 575-646-4346. Fax: 575-646-7706. E-mail: sdeng@nmsu.edu.

Separation of carbon monoxide from gas mixtures by physical adsorption in a pressure swing adsorption process (PSA) was commercialized about 20 years ago.[15−18] The CuCl π-complexation adsorbent was employed in the PSA process for recovering carbon monoxide from syngas.[15−18] Typically, activated alumina, activated carbon, and zeolite are used as supports for dispersing active species CuCl or $AgNO_3$ to form the π-complexation adsorbents. Table 1 summarizes the published carbon monoxide adsorption equilibrium data at given experimental conditions on CuCl π-complexation adsorbents and other physical adsorbents.[15−24] Most of the published carbon monoxide adsorption data only include the equilibrium, only a few reported adsorption kinetics,[25] or heat of adsorption.[23,26,27]

The objective of this study is to compare the adsorption equilibria and kinetics of carbon monoxide on two classical adsorbents zeolite 5A and 13X and two newly discovered adsorbents MOF-5 and MOF-177. Adsorption equilibria and kinetics on these four adsorbents were measured at three temperatures and carbon monoxide pressures up to 108 kPa, which allow us to compare the performance of these adsorbents at identical conditions. The heat of adsorption was determined from the adsorption equilibrium data at different temperatures, and the diffusivity of carbon monoxide in these adsorbents was obtained from the adsorption kinetics data. These data will provide necessary information for adsorbent selection and process design for the PSA processes for carbon monoxide separation and recovery; they will help us understand adsorption fundamentals.

2. Experimental Section

The two zeolite samples (5A and 13X) were kindly provided by Mr. Li Shenan of Nanjing Refinery, SINOPEC, China.

2.1. Syntheses of MOF-5 and MOF-177. The MOF-5 and MOF-177 were synthesized in our laboratory, and a brief description of the synthesis procedures is given below.

The synthesis procedures of MOF-5 and MOF-177 were followed from previous publications.[28−30] For the MOF-5

10.1021/je9000087 CCC: $40.75
Published on Web 05/08/2009

Table 1. Summary of Published Carbon Monoxide Adsorption Equilibrium Data

adsorbents	adsorption condition	adsorption amount or Henry's constant	refs
CuCl/NaY	70 kPa, 30 °C	2.4 mmol·g^{-1}	15
Linde Zeolite 5A	30 °C	K_H = 6.6 mmol·g^{-1}·atm^{-1}	16 to 18
	2 atm, 30 °C	1.3 mmol·g^{-1}	
CuCl/γ-Al_2O_3	30 °C	K_H = 34.5 mmol·g^{-1}·atm^{-1}	16 to 18
	2 atm, 30 °C	1.0 mmol·g^{-1}	
CuCl/Activated Carbon	30 °C	K_H = 7.5 mmol·g^{-1}·atm^{-1}	16 to 18
	2 atm, 30 °C	1.2 mmol·g^{-1}	
Linde Zeolite 5A	1000 mmHg, 77.3 K	6.7 mmol·g^{-1}	19
Columbia grade L Activated carbon	1793 kPa, 311 K	3.0 mmol·g^{-1}	20
Activated carbon (PCB, Calgon Corp.)	5447 kPa, 296 K	4.73 mmol·g^{-1}	21
Zeolite 10X	264.17 kPa, 172 K	4.75 mmol·g^{-1}	22
CuCl/γ-Al_2O_3	26 °C	K_H = 27 mmol·g^{-1}·atm^{-1}	23
$AgNO_3$/γ-Al_2O_3	26 °C	K_H = 32 mmol·g^{-1}·atm^{-1}	23
Al-pillared montmorillonite clay minerals	4 kPa, 20 °C	0.036 mmol·g^{-1}	24

synthesis, all the chemicals were purchased from Fisher Scientific, and they are of the highest available commercial purity (99+ %, except zinc nitrate hexahydrate of 98 % purity). Amounts of 0.832 g of zinc nitrate hexahydrate and 0.176 g of benzene dicarboxylic acid were dissolved in 20 mL of *N*,*N*-diethylformamide (DEF) under constant agitation under atmospheric conditions. The resulting mixture was first degassed thrice using the freeze−pump−thaw method, and then 20 mL reaction vials were filled for crystallization. The capped vials were immediately put in an oven at (85 to 90) °C for crystallization for about 24 h. At the end of the crystallization step, clear golden crystals of MOF-5 emerged from the wall and base of the vials. The MOF-5 crystals were separated from the reaction solution, washed with DEF to remove the unreacted zinc nitrate, and followed by purification in chloroform. The chloroform purification was performed by adding chloroform into 20 mL vials containing the raw MOF-5 crystals. The vials were capped tightly and put back in the oven at 70 °C for another 3 days. Solvent in the vials was replenished with fresh chloroform every day. After the chloroform treatment, the MOF-5 crystals changed from a golden color to transparent. Because MOF-5 crystals are very susceptible to moisture and air, they have to be stored in chloroform or under vacuum in a Schlenk flask.

The synthesis of MOF-177 can be divided into two steps: synthesis of the benzene tribenzoate (BTB) ligand and formation of MOF-177. The BTB ligand was synthesized in our laboratory following the procedures reported by Yaghi et al.[29] To produce MOF-177, 0.32 g of zinc nitrate hexahydrate and 0.07 g of BTB ligand were dissolved in 20 mL of dimethyl formamide. The mixture was degassed thrice using the freeze−pump−thaw method and then stored in a 20 mL reaction vial that was fully filled with the mixture and capped tightly. The vial was then put in an oven at 67 °C for 7 days. At the end of this step, clear and transparent MOF-177 formed and became visible in the wall as well as on the base of the vial. The vial was then removed from the oven, decanted, and washed with dimethyl formamide to remove the unreacted zinc nitrate. The raw MOF-177 crystals were then purified by the chloroform treatment process employed for MOF-5 crystal purification and stored in chloroform or in a Schlenk flask under vacuum as MOF-177 is vulnerable to humid air.

2.2. Adsorption Measurement. Equilibrium and kinetics of carbon monoxide adsorption in all adsorbents were measured volumetrically in a Micromeritics ASAP 2020 adsorption apparatus. Adsorption isotherms were measured at three temperatures, (194.5, 237, and 298) K and up to ambient pressure (~108 kPa). The temperature of the sample bath was constantly monitored with the help of a thermocouple, and it was observed that a temperature variation was no more than ± 0.5 K during the whole experiment. Temperatures of (194.5, 237, and 298) K were achieved by using dry ice, the freezing point of a certain brand of commercially available lubricant oil, and room temperature, respectively. Kinetic data were recorded during isotherm measurements at 298 K and four different pressures. Zeolite 5A and 13X were degassed for 12 h at 623 K, and the MOF samples were degassed at 383 K for 10 h before the adsorption measurements. High purity carbon monoxide (99.99 %) was introduced into a gas port of the adsorption unit for the adsorption measurements. An automatic CO detector was employed during exposure to CO, which was designed to give an alarm when the CO concentration goes above the personal exposure limit (50 ppm). Each adsorption experiment was repeated twice, and no more than ± 2 % variation of data was observed for the entire set of experiments.

3. Results and Discussion

3.1. Adsorption Equilibrium. Adsorption isotherms of carbon monoxide in zeolite 5A, 13X, MOF-5, and MOF-177 at (194.5, 237, and 298) K are plotted in Figures 1a, b, c, and d. It was observed that at room temperature (298 K) and carbon monoxide pressure of 108 kPa zeolite 5A had the highest adsorption amount of 1.22 mmol·g^{-1}, followed by zeolite 13X with a capacity of 0.48 mmol·g^{-1}. However, at 237 K and at 194.5 K and 108 kPa, MOF-177 had the highest adsorption amounts, (3.0 and 4.64) mmol·g^{-1}, respectively.

The Langmuir and Freundlich isotherm models were used to correlate the adsorption isotherms. The Langmuir isotherm is written as

$$q = \frac{a_m bp}{1 + bp} \tag{1}$$

where q (mmol·g^{-1}) is the adsorbed carbon monoxide amount; p is the CO pressure (kPa); a_m (mmol·g^{-1}) is the monolayer adsorption capacity; and b (kPa^{-1}) is the Langmuir adsorption equilibrium constant. Both equation parameters can be determined from the slope and intercept of a linear Langmuir plot of (1/q) versus (1/p).

The Freundlich isotherm is given by

$$q = kp^{1/n} \tag{2}$$

where k and n are the Freundlich isotherm equation parameters that can be determined by the slope and intercept of an ln p versus ln q plot. Table 2 summarizes the isotherm model parameters along with their corresponding absolute relative error (ARE) values.

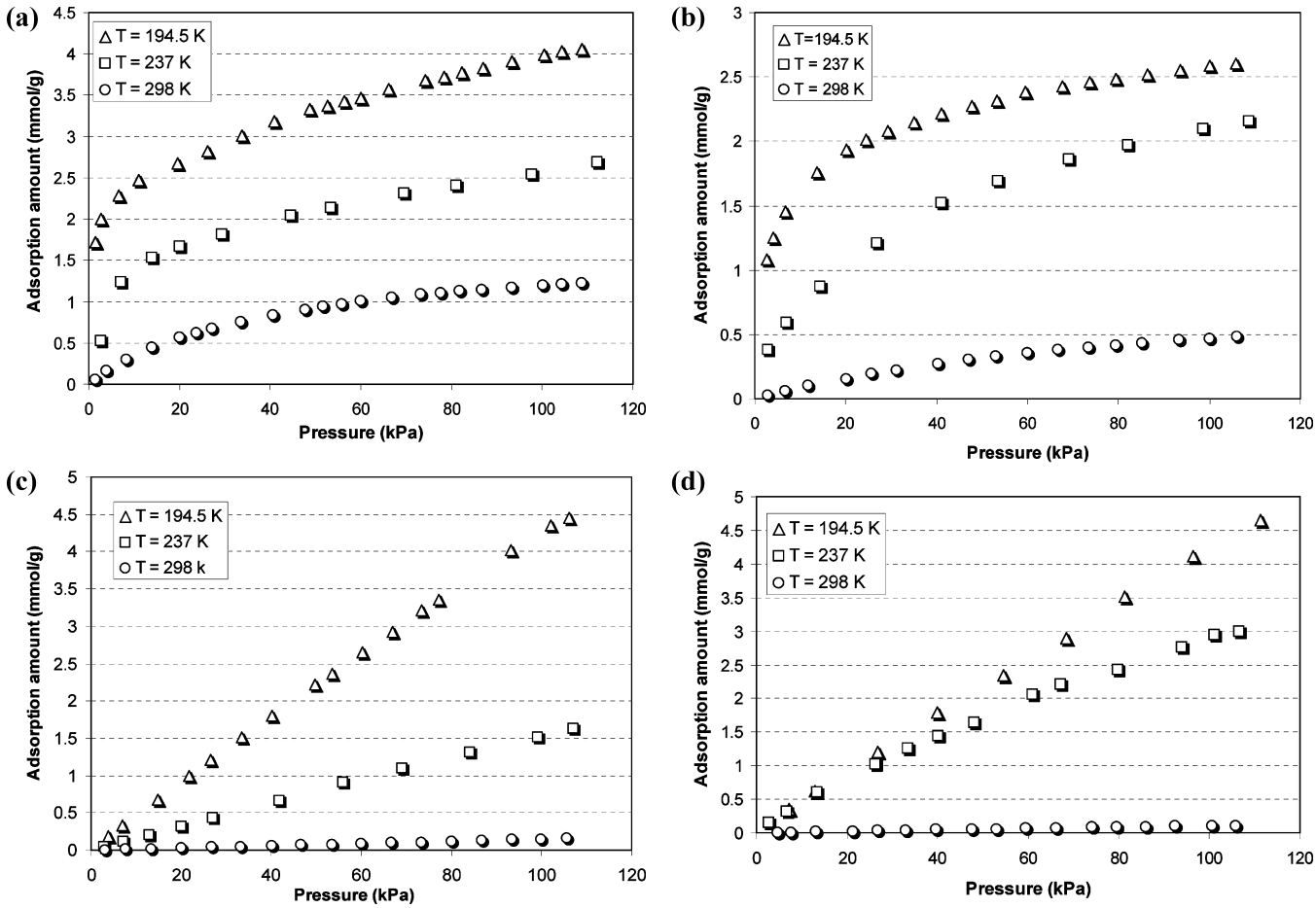

Figure 1. Carbon monoxide adsorption isotherms on (a) zeolite 5A, (b) zeoltie 13X, (c) MOF-5, and (d) MOF-177.

Table 2. Equation Constants for the Langmuir and Freundlich Isotherm Models

adsorbents	temperature(K)	Langmuir model parameters		ARE %	Freundlich model parameters		ARE %
Zeolite 5A	298	a_m	5.28	4.66	k	0.046	11.61
		b	0.0028		n	1.49	
	237	a_m	7.67	5.30	k	1.19	0.98
		b	0.01		n	3.68	
	194.5	a_m	9.76	10.04	k	2.97	2.2
		b	0.08		n	5.11	
13X	298	a_m	2.72	0.37	k	0.007	6.51
		b	0.001		n	1.25	
	237	a_m	5.51	11.96	k	0.244	3.42
		b	0.01		n	2.050	
	194.5	a_m	6.86	5.53	k	1.65	2.4
		b	0.03		n	4.4	
MOF-5	298	a_m			k	$5 \cdot 10^{-4}$	2.12
		b			n	1	
	237	a_m			k	$6 \cdot 10^{-3}$	1.66
		b			n	1.02	
	194.5	a_m	93.45	1.17	k	0.02	0.81
		b	$2 \cdot 10^{-4}$		n	1.03	
MOF-177	298	a_m			k	$2 \cdot 10^{-4}$	7.71
		b			n	0.91	
	237	a_m	13.53	6.06	k	0.03	3.04
		b	$1.4 \cdot 10^{-3}$		n	1.21	
	194.5	a_m	61.34	2.52	k	0.022	0.79
		b	$3 \cdot 10^{-4}$		n	1.05	

The adsorption isotherms of carbon monoxide on zeolite 5A and 13X are of a typical type I isotherm, suggesting strong interaction between the zeolites and carbon monoxide. There is a small dipole moment in the carbon monoxide molecule with the negative end on the carbon atom that may be strongly attracted to the cations in the zeolite. However, the carbon monoxide isotherms on MOF-5 and MOF-177 are quite linear, demonstrating a weak interaction between carbon monoxide and MOFs. The higher adsorption capacity on MOF-5 and MOF-177 at 237 K and at 194.5 K and 108 kPa is attributed to the much larger specific surface area of MOF-5 (BET of 2449 $m^2 \cdot g^{-1}$)[28] and MOF-177 (BET of 3275 $m^2 \cdot g^{-1}$)[30] than those of zeolite 5A and 13X. The values of heat of adsorption of carbon monoxide on zeolites and MOFs

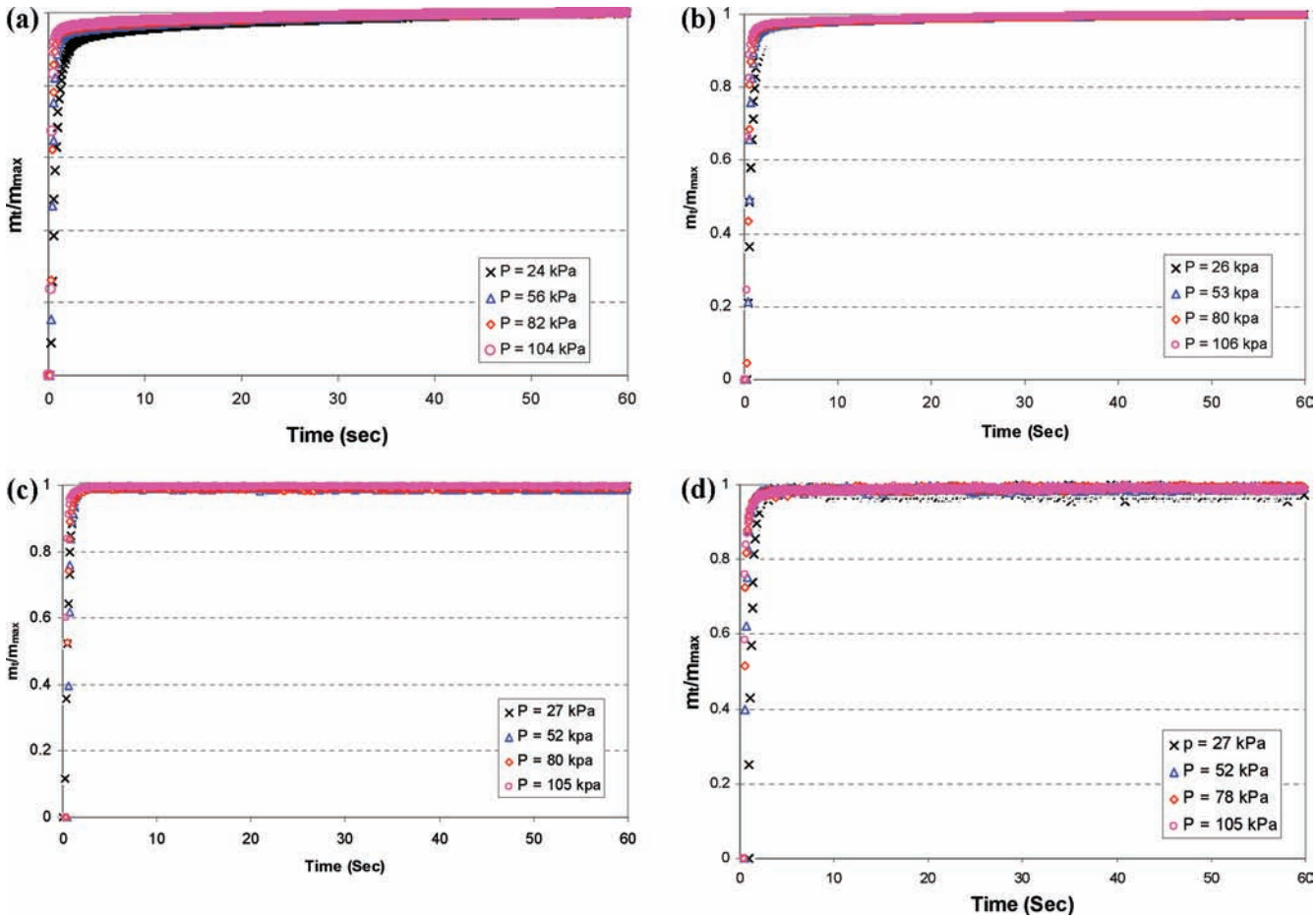

Figure 2. Carbon monoxide adsorption uptake curves at 298 K on (a) zeolite 5A, (b) zeoltie 13X, (c) MOF-5, and (d) MOF-177.

presented in section 3.3 confirm the stronger interactions between carbon monoxide and zeolites and weaker interactions between carbon monoxide and MOFs.

3.2. Adsorption Kinetics. Adsorption kinetics data of carbon monoxide on the four adsorbents were collected at the same time when the isotherms were measured at 298 K in a Micromeritics ASAP 2020 adsorption unit. Kinetic uptake curves for these adsorbents at four different pressure levels are shown in Figure 2a, b, c, and d. It is clear that MOF-5 and MOF-177 reached the adsorption saturation level in a shorter interval of time (within 5 s) in comparison to zeolite 5A or 13X (within 20 s). A classical micropore diffusion model was applied to correlate the adsorption kinetics data and to extract the intracrystalline diffusivity for carbon monoxide in these adsorbents. The fractional adsorption uptake (m_t/m_∞) can be correlated with the diffusion time constant by the following equation if the fractional adsorption uptake is greater than 70 %.[31]

$$1 - \frac{m_t}{m_\infty} = \frac{6}{\pi^2} \exp\left(\frac{-\pi^2 D_c t}{r_c^2}\right) \qquad (3)$$

The diffusion time constants (D_c/r_c^2, s^{-1}) were calculated from the slope of a linear plot of $\ln(1 - (m_t/m_\infty))$ versus t (time) at a given CO pressure. Only data points with (m_t/m_∞) greater than 70 % and less than 99 % were used for estimating the diffusion time constants. The diffusivity (D_c) of carbon monoxide was calculated from the diffusion time constant. The crystallite radius, r_c, for zeolite 5A and 13X particles was provided by the supplier ($r_c = 2.54 \cdot 10^{-5}$ m, $1.44 \cdot 10^{-5}$ m for 5A and 13X, respectively), and the crystallite radius for MOF-5 and MOF-177 ($r_c = 9.31 \cdot 10^{-5}$ m, $1.2 \cdot 10^{-4}$ m for MOF-5 and MOF-177, respectively) was estimated from their SEM images reported in our previous research.[28,30] The average diffusivities of carbon monoxide are $3.42 \cdot 10^{-11}$ $m^2 \cdot s^{-1}$, $1.40 \cdot 10^{-11}$ $m^2 \cdot s^{-1}$, $1.72 \cdot 10^{-8}$ $m^2 \cdot s^{-1}$, and $5.01 \cdot 10^{-9}$ $m^2 \cdot s^{-1}$ for zeolite 5A, 13X, MOF-5, and MOF-177, respectively.

The plots of variation of diffusivity with adsorbate pressure or adsorption amount for zeolite 5A, 13X, are shown in Figure 3a, and those for MOF-5 and MOF-177 are shown in Figure 3b. As shown in Figure 3a and b, the carbon monoxide diffusivities in MOF-5 and MOF177 are in the order of (10^{-9} to 10^{-8}) $m^2 \cdot s^{-1}$, and carbon monoxide diffusivities in zeolite 5A and 13X are in the order of 10^{-11} $m^2 \cdot s^{-1}$. It is quite challenging to explain the difference of adsorption kinetics of carbon monoxide in these adsorbents. We hypothesize that the slightly larger pore sizes MOF-5 (8.6 Å) and MOF-177 (12.7 Å) might have facilitated the carbon monoxide diffusion in these MOFs.

It is observed that the carbon monoxide diffusivities in zeolite 13X, MOF-5, and MOF-177 decrease slightly with an increase in carbon monoxide pressure. This is probably attributed to the fact that the adsorbent pores were partially saturated and blocked at higher adsorption loading in the higher pressure range giving rise to sluggish kinetics. The slightly increasing trend observed in zeolite 5A as shown in Figure 3a is possibly due to the surface diffusion of carbon monoxide inside zeolite 5A at high pressures. This is because the kinetic diameter of carbon monoxide is 3.59 Å, which is slightly smaller than the pore diameter of zeolite 5A (4.4 Å). It is expected that the pores of zeolite 5A will be

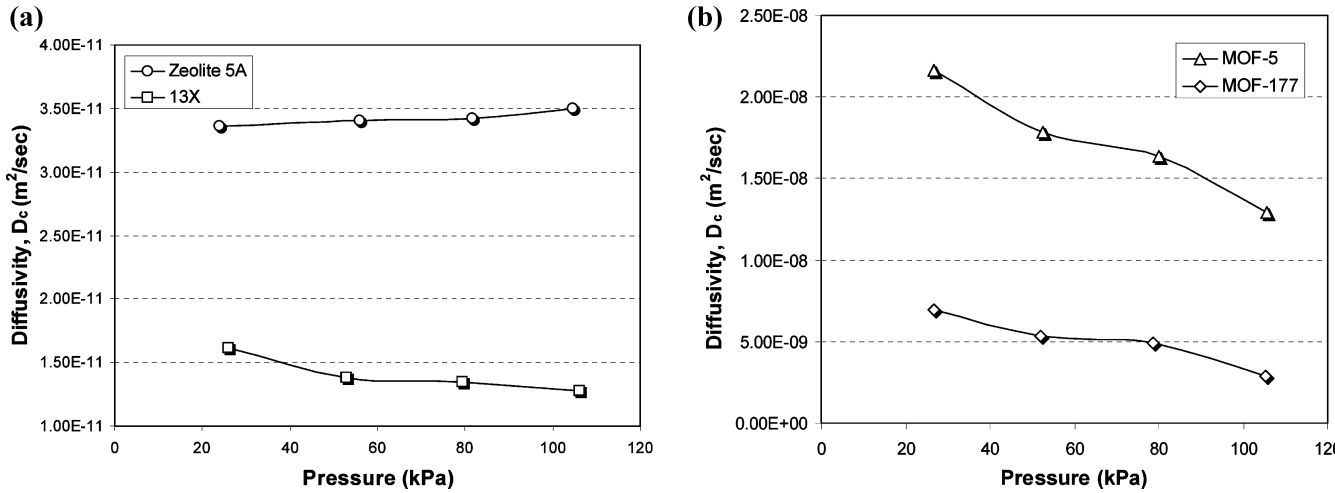

Figure 3. Variation of carbon monoxide diffusivity with pressure at 298 K on (a) zeolite 5A and 13X at 298 K and (b) MOF-5 and MOF-177.

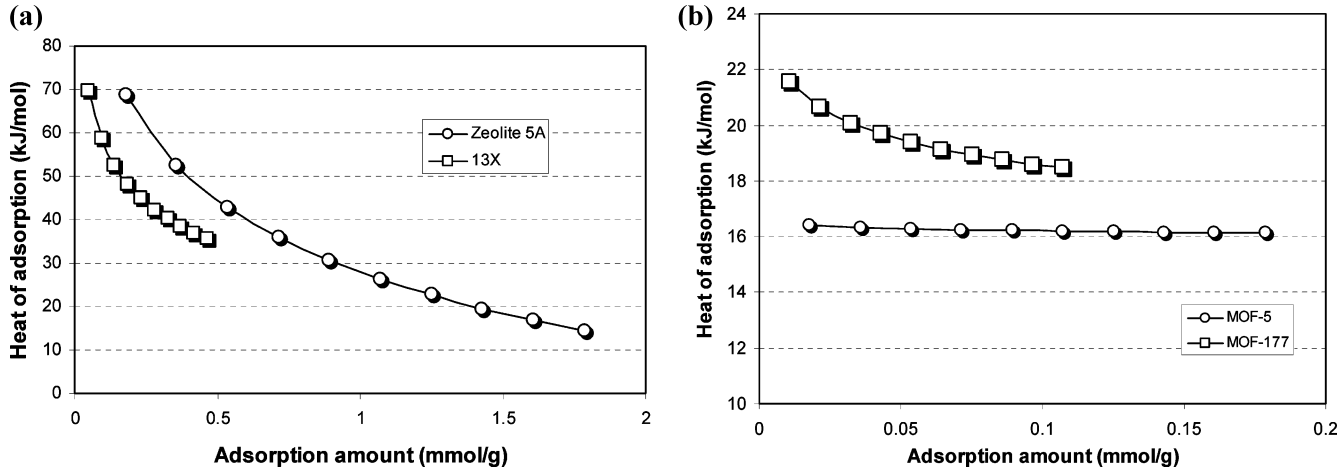

Figure 4. Heat of adsorption of carbon monoxide on (a) zeolite 5A and 13X and (b) MOF-5 and MOF-177.

blocked after adsorption at a very low pressure, so the decreasing trend of diffusivity with pressure observed in zeolite 13X, MOF-5, and MOF-177 could not be measured at the experimental conditions used in this work. The surface diffusion due to a higher adsorption capacity of carbon monoxide on zeolite 5A at a higher pressure plays a major role, which leads to a slight increase in diffusivity at higher pressures.

3.3. Isosteric Heat of Adsorption. Isosteric heat of adsorption is also an important parameter for gas separation through physical adsorption. The isosteric heat of adsorption can be obtained from the van't Hoff's equation

$$\frac{\Delta H}{RT^2} = -\left(\frac{\partial \ln p}{\partial T}\right)_a \tag{4}$$

where ΔH is the isosteric heat of adsorption (kJ·mol^{-1}); T is temperature; p is pressure (bar); a is the adsorption amount (mmol·g^{-1}); and R is the universal gas constant. Integration of eq 4 gives

$$\ln P = \frac{\Delta H}{RT} + C \tag{5}$$

where C is an integration constant.

In the present study, three carbon monoxide adsorption isotherms at (194.5, 237, and 298) K were used to calculate the heat of adsorption plots. The measurement points were achieved by employing the suitable model fitting equation (i.e., Langmuir or Freundlich). The adsorption isotherms were first converted to adsorption isosteres, a plot of ln p versus $1/T$ at a given adsorption amount. The heat of adsorption was then calculated from the slopes of the isosteres according to eq 5. The plots of the variation of heat of adsorption with the adsorption amount for zeolite 5A and 13X are shown in Figure 4a, and those for MOF-5 and MOF-177 are shown in Figure 4b. The values of heats of adsorption for carbon monoxide for zeolite 5A and 13X decrease significantly with the adsorption amount, and the maximum value of 70 kJ·mol^{-1} was observed at the lowest adsorption loading. This value (70 kJ·mol^{-1}) is higher than the value measured in CuCl or $AgNO_3$ doped γ-Al_2O_3 (48 kJ·mol^{-1}),[23] H-ZSM-5 (33.4 kJ·mol^{-1}),[25] but is close to that measured on cuprous amine doped Y zeolite (79.5 kJ·mol^{-1}).[26] It is interesting to observe that the heat of adsorption in MOF-5 does not change with the adsorption amount, and the heat of adsorption of carbon monoxide in MOF-177 decreases with the adsorption amount. The heats of adsorption in MOF-5 (16 kJ·mol^{-1}) and MOF-177 (< 22 kJ·mol^{-1}) are relatively smaller than those in the zeolite 5A and 13X. These values confirm the stronger interactions between carbon monoxide and zeolites 5A and 13X than those between carbon monoxide and MOFs as observed in the carbon monoxide adsorption isotherms.

4. Conclusion

Adsorption equilibria and kinetics of carbon monoxide on zeolite 5A, 13X, MOF-5, and MOF-177 were measured at (298,

237, and 194.5) K and carbon monoxide pressures up to 108 kPa. It was observed that zeolite 5A had the highest adsorption amount of 1.22 $mmol \cdot g^{-1}$ at ambient temperature (298 K) and ambient pressure (108 kPa), and MOF-177 has a higher carbon monoxide adsorption capacity at (194.5 and 237) K. Carbon monoxide diffusivity decreases with the adsorption amount in all adsorbents except for zeolite 5A. The surface diffusion of carbon monoxide makes the diffusivity increase with the adsorption amount in zeolite 5A. The average carbon monoxide diffusivities at 298 K and carbon monoxide pressures below 108 kPa are $3.42 \cdot 10^{-11}$ $m^2 \cdot s^{-1}$, $1.40 \cdot 10^{-11}$ $m^2 \cdot s^{-1}$, $1.72 \cdot 10^{-8}$ $m^2 \cdot s^{-1}$, and $5.01 \cdot 10^{-9}$ $m^2 \cdot s^{-1}$ for zeolite 5A, 13X, MOF-5, and MOF-177, respectively. It was also observed that the heat of adsorption decreases with the adsorption amount for all adsorbents except MOF-5. The heat of adsorption of carbon monoxide at low coverage in zeolite 5A and 13X is below 70 $kJ \cdot mol^{-1}$ and decreases sharply with the adsorption amount, while the heat of adsorption of carbon monoxide in MOF-5 and MOF-177 is in the range of (16 to 22) $kJ \cdot mol^{-1}$.

Literature Cited

(1) Sing, B.; Saxena, A.; Srivastava, A. K.; Vijayaraghavan, R. Impregnated carbon based catalyst for protection against carbon monoxide gas. *Appl. Catal., B: Environ.* **2008**, doi:10.1016/j.apcatb (in press).

(2) International Organization for Standardization "Hydrogen fuel -- Product specification -- Part 2: Proton exchange membrane (PEM) fuel cell applications for road vehicles", ISO/TS 14687−2:2008, March 1, 2008.

(3) Larminie, J.; Dicks, A. *Fuel Cell Systems Explained*, 2nd ed.; Wiley: New York, 2003.

(4) Noyes, W. A., Jr.; Washington, D. C. Summary Technical report of the National Defense Research Committee Division 10, 1946.

(5) Beebe, R. A.; Wildner, E. L. The Heat of Adsorption of Carbon Monoxide on Copper. *J. Am. Chem. Soc.* **1934**, *56* (3), 642–645.

(6) Wadeyama, T.; Osano, H.; Oda, S.; Todoroki, N. ; Carbon monoxide adsorption on Pd-deposited Cu(1 1 0) surface: Infrared reflection adsorption and temperature programmed desorption studies. *Appl. Surf. Sci.* **2008**, *254*, 5380–5384.

(7) Taylor, H. S.; McKinney, P. V. Adsorption and activation of carbon monoxide at palladium surfaces. *J. Am. Chem. Soc.* **1931**, *53* (10), 3604–3624.

(8) Sastri, M. V. C.; Viswanathan, T. S.; T. S. Nagarjunan, T. S. The influence of a chemisorbed layer of carbon monoxide on subsequent physical adsorption. *J. Phys. Chem.* **1959**, *63* (4), 518–521.

(9) Tseng, C. H.; Yang, T. C. K.; Wu, H. E. Catalysis of oxidation of carbon monoxide on supported gold nanoparticle. *J. Hazard. Mater.* **2009**, in press.

(10) Skurnik, S.; Steiburg, M. Heat of adsorption of carbon monoxide on coprecipitated nickel oxide-silica catalyst. *I EC Fundam.* **1967**, *6* (3), 459–460.

(11) Morishige, K.; Tomoyasu, S.; Iwano, G. Adsorption of CO, O_2, NO_2, and NH_3 by Metallophthalocyanine Monolayers Supported on Graphite. *Langmuir* **1997**, *13*, 5184–5188.

(12) Probst, R. E.; Meyerson, S.; Seelig, H. S. Adsorption and reaction of carbon monoxide on promoted iron catalyst. *J. Am. Chem. Soc.* **1952**, *74* (8), 2115–2116.

(13) Smart, R. S. C.; Slager, T. L.; Little, L. H.; Greenler, R. G. Carbon monoxide adsorption on magnesium oxide. *J. Phys. Chem.* **1973**, *77* (8), 1019–1023.

(14) Burwell, R. L., Jr.; Taylor, H. S. The adsorption and decomposition of carbon monoxide on the zinc oxide catalysts. *J. Am. Chem. Soc.* **1937**, *59* (4), 697–699.

(15) Xie, Y. C.; Zhang, J.; Qiu, J.; Tong, X.; Fu, J.; Yang, G.; Yan, H.; Tang, Y. Q. Zeolites modified by CuCl for separating CO from gas mixtures containing CO_2. *Adsorption* **1996**, *3*, 27–32.

(16) Golden, T. C.; Kratz, W. C.; Wilhelm, F. C. Highly dispersed cuprous compositions, U.S. Patent 5,126,310, 1992.

(17) Golden, T. C.; Kratz, W. C.; Wilhelm, F. C.; Pierantozzi, R.; Rokicki, A. Highly dispersed cuprous compositions, U.S. Patent, 5,175,137, 1992.

(18) Golden, T. C.; Guro, D. E.; Kratz, W. C.; Occhialini, J. M.; Sabram, T. E. *Fundamentals of Adsorption*; Elsevier: Amsterdam, The Netherlands, 1998.

(19) Flock, J. W.; Lyon, D. N. Adsorption isotherms, heats of desorption, and partial molal entropies for carbon monoxide on Linde 5A molecular sieve. *J. Chem. Eng. Data* **1974**, *19*, 205–209.

(20) Ray, G. C.; Box, E. O. Adsorption of gases on activated charcoal. *Ind. Eng. Chem.* **1950**, *42* (7), 1315–1318.

(21) Ritter, J. A.; Yang, R. T. Equilibrium adsorption of multicomponent gas mixtures at elevated pressures. *Ind. Eng. Chem. Res.* **1987**, *26* (8), 1679–1686.

(22) Nolan, J. T.; Mckeehan, T. W.; Danner, R. P. Equilibrium adsorption of oxygen, nitrogen, carbon monoxide, and their binary mixtures on molecular sieve type 10X. *J. Chem. Eng. Data* **1981**, *26* (2), 112–115.

(23) Deng, S.; Lin, Y. S. Sol-Gel Preparation and Properties of Alumina Adsorbents for Gas Separation. *AIChE J.* **1995**, *41* (3), 559–570.

(24) Itadani, A.; Tanaka, M.; Abe, T.; Taguchi, H. Mahiko Nagao, Al-pillared montmorillonite clay minerals: Low-pressure CO adsorption at room temperature. *J. Colloid Interface Sci.* **2007**, *313*, 747–750.

(25) Stanislaus, A.; Evans, M. J. B.; Mann, R. F. Kinetics of adsorption of carbon monoxide on alumina. *J. Phys. Chem.* **1972**, *76* (17), 2349–2352.

(26) Szanyi, J.; Paffett, M. T. The adsorption of carbon monoxide on H-ZSM-5 and hydrothermally treated H-ZSM-5. *Microporous Mater.* **1996**, *7*, 201–218.

(27) Huang, Y. Y. Selective adsorption of carbon monoxide and complex formation of cuprous amines in Cu(I) Y zeolites. *J. Catal.* **1973**, *30*, 187–194.

(28) Saha, D.; Wei, Z.; Deng, S. Hydrogen adsorption equilibrium and kinetics in metal-organic framework (MOF-5) synthesized with DEF approach. *Sep. Purif. Technol.* **2009**, *64*, 280–287.

(29) Furukawa, H.; Miller, M. A.; Yaghi, M. Independent verification of the saturation hydrogen uptake in MOF-177 and establishment of a benchmark for hydrogen adsorption in metal- organic frameworks. *J. Mater Chem.* **2007**, *17*, 3197–3204.

(30) Saha, D.; Wei, Z.; Deng, S. Equilibrium, kinetics and enthalpy of hydrogen adsorption in MOF-177. *Int. J. Hydrogen Energy* **2008**, *33*, 7479–7488.

(31) Ruthven D. M. *Principles and adsorption and adsorption processes*; Willey Interscience: New York, 1984.

Received for review January 3, 2009. Accepted April 15, 2009.

JE9000087